Article

Journal of
Nanoscience and Nanotechnology
Vol. 15, 1045–1052, 2015
www.aspbs.com/jnn

Copyright © 2015 American Scientific Publishers
All rights reserved
Printed in the United States of America

Nanodiamonds of Laser Synthesis for Biomedical Applications

E. Perevedentseva[1, 2], D. Peer[3], V. Uvarov[4], B. Zousman[5], and O. Levinson[5, *]

[1] IR Lab, Department of Physics, National Dong Hwa University, 974, Taiwan
[2] P. N. Lebedev Physical Institute of the Russian Academy of Sciences, Moscow, 119991, Russia
[3] Laboratory of NanoMedicine, Center for Nanoscience and Nanotechnology, Department of Cell Research and Immunology and Department of Materials Science and Engineering, Tel-Aviv University, 6139001, Israel
[4] The Center for Nanoscience and Nanotechnology, The Hebrew University of Jerusalem, 9190401, Israel
[5] Ray Techniques Ltd., Jerusalem, 9139101, Israel

In recent decade detonation nanodiamonds (DND), discovered 50 years ago and used in diverse technological processes, have been actively applied in biomedical research as a drug and gene delivery carrier, a contrast agent for bio-imaging and diagnostics and an adsorbent for protein separation and purification. In this work we report about nanodiamonds of high purity produced by laser assisted technique, compare them with DND and consider the prospect and advantages of their use in the said applications.

Keywords: Nanodiamond, Synthesis, Laser Ablation, Biomedicine, Toxicity.

1. BACKGROUND

Having been discovered in Russia in 1963 by Danilenko and co-workers,[1] nanodiamonds (ND) have been studied, produced on commercial scale and applied in industry, mostly in lubricating, polymer composites, fine polishing and diverse coatings. Highly promising results of experiments in various fields, such as energy storage,[2] quantum computing,[3] catalysis in chemical processes,[4] heat conductive insulating compounds[5] and other novel composite materials with improved properties have been obtained and characterized in recent years. Particular place in this long list of developing applications belongs to biomedical research. Unique combination of features: variability of particle size from a few to hundreds nanometers, mechanical hardness, presence of surface shell of alterable functional groups enabling desired interaction with bio-molecules, large specific surface area, high adsorption potential, stable photo-luminescence, chemical inertness and non-cytotoxicity, makes nanodiamonds highly promising to be used in biological applications, in drug and gene delivery, separation and purification of proteins and DNA immobilization, bio-imaging and diagnostics.[6–8]

Substantial progress has been made recently in the using nanodiamond fluorescence[6, 9] and Raman signal[9] for the imaging and drug delivery tracking. This is because nanodiamonds allow staining bio-objects, e.g., cells, and act as stable non-photobleaching labels. Nanodiamond surface functionalization by the attaching various molecules of interest for interaction with biological targets allows to use nanodiamonds not only for specific interaction for imaging, but also for delivery of drugs, genes and some other materials.[7–9] At the same, nanodiamond biocompatibility has been confirmed for number of cell cultures and currently is studied for higher levels of bio-system organization.[6, 8, 9] In addition, presently novel nanodiamond bio-applications are discussed, such as the using multi-photon excitation[10] and optically detected magnetic resonance for imaging,[11] as well as the development of multifunctional fluorescent composite bone scaffold material based on biodegradable polymer and functionalized fluorescent nanodiamonds.[12]

However, in spite of obvious advantages of nanodiamonds in biomedicine comparing with other nanoparticles, significant efforts and funds spent for the development of new formulations and a lot of exciting results reported, to the best of our knowledge, any implementation has not been achieved in industrial scale. In general, this is caused

*Author to whom correspondence should be addressed.

by drawbacks of the existing methods of synthesis and the features of nanodiamond particles produced by the existing technologies: high-temperature and high-pressure (HTHP) and detonation.

2. PROBLEMS WITH USE OF NANODIAMONDS IN BIO-MEDICINE

HTHP: Diamond micro-crystals are produced at the conditions of constant temperature and pressure high enough for the converting carbon atoms of graphite into diamond structure.[13] To be used in bio-applications, obtained microdiamonds undergo crushing and fractionation resulting in nanodiamonds with the size from of 40 to hundreds nm (HTHP ND). These particles usually have good diamond structure with insignificant surface of non-diamond fraction,[14] with well detectable photoluminescence (from defect color centers embedded in diamond structure)[15] and surface chemistry, which can be controlled by different functionalization methods.[16] Low cytotoxicity for many kinds of cells, as well as for multicellular organisms (e.g., worms) has been demonstrated.[17] *In-vivo* studies on animals confirm that these nanodiamonds are collected in the organism and the ways of their release are not clear yet. Moreover, the big size of HTHP ND, as well as wide size distribution and irregular shape of the particles can limit their cellular applications, so the combination of their advantages with decreased size would open new opportunities for their application in bio-medicine. Therefore, nanodiamonds with significantly smaller dimensions have been intently studied in recent years.

Detonation: Detonation nanodiamonds (DND) are produced by detonating explosives (mainly trotyl and hexogen) with negative oxygen balance in big metallic chambers.[6] During the explosion, the pressure and temperature in the chamber become high enough to convert the carbon of the explosives into crystallites with average size of 4–5 nm with cubic structure. Wide spectrum of synthesis conditions for diverse diamond nanoparticles synthesized by detonation results in wide variability of sizes, structure features and surface chemistry, which usually affects different reactivity and complexity of implementation in industrial scale for most applications.

The problems which now limit further development of biomedical DND applications are first of all their aggregation, badly controllable surface chemistry and low spectroscopic signals. As a result, the aggregation limits the obtaining particles with controllable size and shape, as well as surface properties. Also desired interaction with bio-molecules is significantly restricted. The attempts to solve this problem included development of various methods of disaggregation, including varying zeta-potential,[18] stirred-media milling,[19, 20] subjecting the suspension to shock waves[21] and high temperature graphitization with following oxidizing,[22] ultrasound treatment[23, 24] but the problem still exists, mainly because of a non-constant reactivity of DND, caused by uncontrollable character of the detonation technology.

Both aggregation and surface chemistry can be responsible for lower biocompatibility of DND[17] in comparison with HTHP ND. On the other hand, big surface area and controllable surface chemistry are significant advantagesfor effective conjugation of nanodiamonds with biomolecules in each concrete application.

The combination of advantages of HTPT ND (their structure and spectroscopic properties) and of DND (small size and chemically active surface) could widen the ND applicability in different fields, first of all, in bio-medical research.

In this paper we describe a new method for the fabrication nanodiamonds by laser assisted technique, compare them with DND and analyze their applicability in biomedicine.

3. NEW METHOD OF SYNTHESIS: LIGHT HYDRO-DYNAMIC PULSE (LHDP)

The developed technology belongs to Pulse Laser Ablation in Liquid (PLAL), also called Pulsed-Laser-Induced liquid–solid Interfacial Reaction (PLIIR) or Liquid Phase Pulse Laser Ablation (LP-PLA), the method firstly applied for nanoparticles synthesis in 1987.[25] After that various nanomaterials were produced by PLAL: silver, gold, CBN, titanium dioxide, cobalt oxide, cubic-carbon nitride and other.[26] In 1998 obtaining nanodiamonds by ablation of graphite solid target in water was reported.[27] Since then several academic groups have investigated this process and obtained nanodiamonds of diverse sizes using pulse laser YAG of various power and wave length. However, the researchers had to admit, that in spite of the obvious advantages-high purity of obtained powder and controlled character of the synthesis–the process is uneconomical and cannot compete with the existing technologies of synthesis because of too low output. Two main novelties proposed by the authors: using a special multi-component target for laser treatment instead of graphite and focusing a laser beam on some predicted distance from the target and not on the surface, changed the conditions of nanodiamonds formation and resulted in significant increase of the output. The synthesis occurs as a result of light-acoustic shock wave treatment and not of plasma impact, as happens in traditional PLAL. On the other hand, varying of the parameters of the synthesis enables not only to enhance the yield of produced nanodiamonds but also to control the properties of synthesized nanodiamonds. All this opens the prospect of the implementation of the technology in industrial scale and its competiveness against the existing method of detonation synthesis. The new approach is based on Light Hydro-Dynamic Effect[28] and Effect of Self-Focusing Optical Beams[29] discovered in Soviet Union in the 60s. It was found that high-power laser radiation beam passing through a fluid changes its optical properties

and converges focusing on some point causing a flash of white light and acoustic wave and resulting in hydro-shock of extremely high power.[30] Herewith, by the varying of laser radiation parameters, a refractive index of the media, a composition of special target and a distance from the focus to the target, it is possible to find such conditions of a temperature and a pressure, in which carbon atoms are bonded in three-dimensional cubic lattice forming diamond nano-crystals with dimensions and a surface chemistry suitable for further applications.

Since LHDP technology opens the prospect of obtaining small nanodiamonds required for bio-medicine, the comparative analysis of ND obtained by laser synthesis (LND) and commercially available DND is an actual issue.

4. NANODIAMOND CHARACTERIZATION

Samples for comparison

1. LND, nanodiamond powder produced by LHDP. Specially prepared target was obtained by mixing of 50% pure carbon soot and 50% hydrocarbon, scanning step of 20 μm, laser wave length: 1064 nm.
2. DND purchased from Alit, Ukraine

4.1. X-Ray Diffraction Analysis

X-ray powder diffraction measurements were performed on the D8 Advance diffractometer (Bruker AXS, Karlsruhe, Germany) with Gobel mirror parallel beam optics, 2° Sollers slits and 0.2 mm receiving slit. Low-background quartz sample holders were carefully filled with the powder samples. XRD patterns within the range 10° to 95° 2θ were recorded at room temperature using CuKα radiation ($\lambda = 1.5418$ Å) with following measurement conditions: tube voltage of 40 kV, tube current of 40 mA, step-scan mode with a step size of 0.02° 2θ and counting time of 1 s/step. TOPAS-v.3 (Bruker AXS) software was used for structure refinement. The Scherrer equation was used for crystallite size calculations.[31] The instrumental broadening was determined using LaB_6 powder (NIST-660a).

Figure 1 shows the XRD patterns acquired from as-synthesized ND powders. Careful examination of XRD patters reveals that the peaks' positions and intensities well correspond to diamond (space group Fd-3m, (No. 227), $a = 3.567$ Å, PDF-03-065-0537). It was found also, that XRD patterns are practically identical and the specimens don't contain an amorphous or other additional crystal phases. We applied Rietveld method for the refinement of the structural parameters. Basic model of cubic diamond structure and Fundamental Parameters Approach for profile fitting were used. The data were corrected for peak asymmetry due to axial divergence.[28] The values of isotropic temperature factors B_{eq} were about 2 Å^{-2} and values of R_{wp} factor were about 14–16% for all the tested samples, and they indicate a good quality of

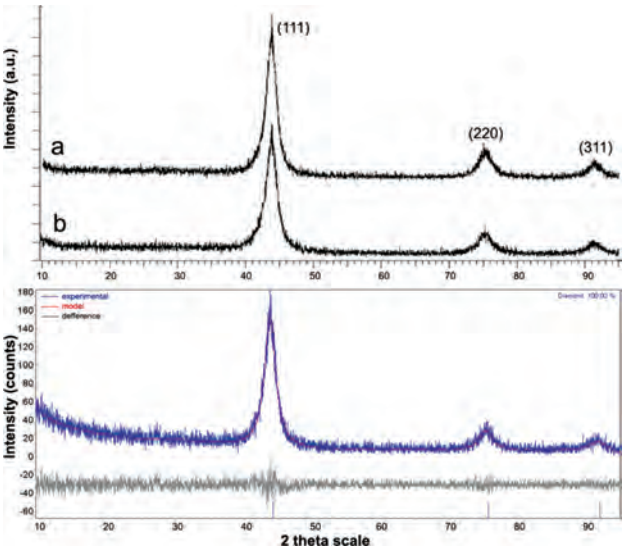

Figure 1. XRD patterns acquired from nanodiamond powders (a)—specimen LND, (b)—specimen DND) (upper) and graphical representation of Rietveld refinement results for nanodiamond synthesized by LHDP method. Peak positions of Diamond are shown by vertical bars (bottom).

Rietveld refinement and reliability of obtained results. The graphical result of the Rietveld refinement also is shown in Figure 1, and the main results are presented in Table I.

Comparison of the data in the Table I confirms that the examined samples of nanodiamond powders both of detonation and laser synthesis have almost identical crystalline characteristics.

4.2. Scanning Electron Microscopy

Morphological observations and identification of the chemical composition were performed with the Extra High Resolution Scanning Electron Microscopy (XHR SEM) Magellan 400L (FEI Company, USA).

SEM images were acquired from commercial DND and synthesized LND powders. As is seen in Figure 2, the powders are composed of nanometer size particles and the particles of both powders have very similar rounded morphology. The average particle size is about 4–5 nm. This size is in good agreement with the XRD results. Being imaged under the same excitation conditions (Figs. 2(c) and (d)) both powders exhibit very similar contrast that could be explained as a result of similar elemental composition.

Table I. Main results of Rietveld refinement of XRD data.

ND type	Unit cell parameter, (Å)	Crystallite size (nm)	Isotropic temperature factors B_{eq} (Å^{-2})	R_{wp} factor at Rietveld refinement, %
LND	3.563 (0.09)	4.64 (0.14)	2.1 (4)	14.2
DND	3.562 (0.12)	5.23 (0.19)	2.3 (2)	16.1

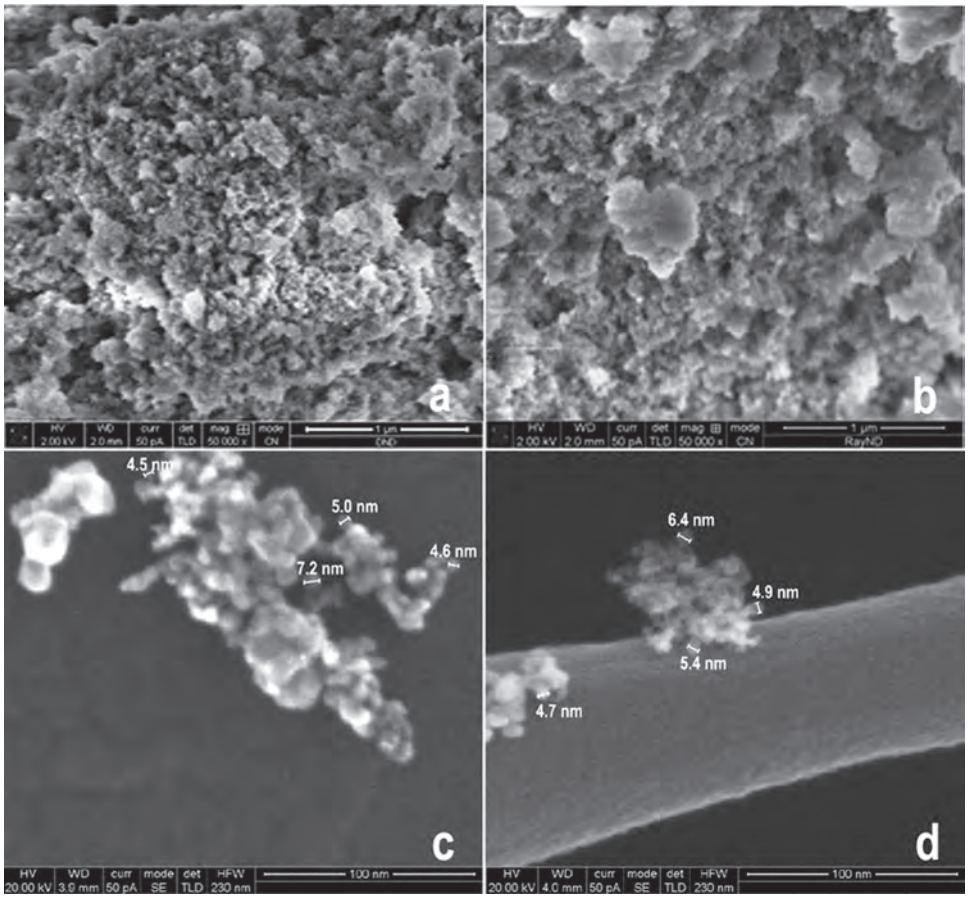

Figure 2. High Resolution SEM images of DND (a) and (c) and LND (b) and (d); the scale bar in (a) and (b) is 1 μm, in (c) and (d) 100 nm.

4.3. Transmission Electron Microscopy

High resolution TEM Tecnai F20 G2 was used to analyze the microstructure of nanodiamond samples. Obtained images and electron diffraction patterns (Fig. 3) show the similar structure and dimensions of the analyzed powders. However, at DND image non-diamond shells can be observed on the grain surface, while the surface of LND particles seams non-coated. Diamond cubic lattice was confirmed by the measuring of interplanar spacing detected by Electron Diffraction. Character of electron ED patterns (presence of continuous rings and absence of strong single spots) testifies that the size of crystallites doesn't exceed 8–10 nm. Additional diffraction rings or spots, which are not related to the diamond, are absent in electron diffraction patterns. It is evidence of high purity of synthesized material.

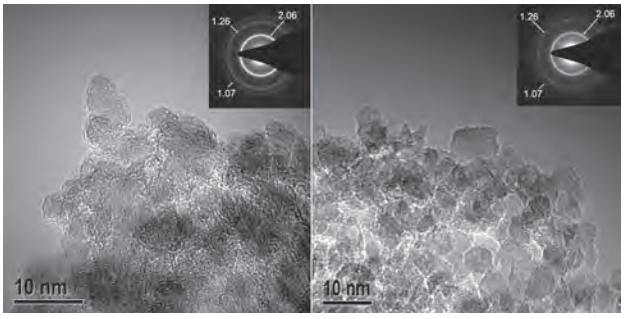

Figure 3. HR TEM images and selected area electron diffraction patterns (SAEDs) (insets) acquired from DND (left) and LND (right) nanodiamond specimens.

Electron Energy Loss Spectroscopy (EELS) (Fig. 4) was used to determine the bonding. EELS spectra of DND and LND look very similar: the pre-peak at the region of 285–290 eV, the core-loss peak and the high peak of 300 eV, then the "sole" and two peaks at the regions of 315 and 335 eV. The small peak in LND sample at the region of 410 eV[32] indicates slight presence of nitrogen vacancy (NV) defects in nanodiamond grains. This peak is not observed in the DND sample. Smaller size of the pre-peak at 285–290 in LND spectrum indicates lower content of non-diamond structure on the surface comparing with DND.

Energy Dispersive X-Ray Spectroscopy (EDS) was performed using HR TEM Tecnai F20 G2, which provides high-resolution performance in micro-analysis and STEM imaging, to determine element content of the powders at chosen areas (Fig. 5). The samples were analyzed without pretreatment. In order to obtain more accurate information, the test was repeated 10 times for both samples, wherein diverse areas around 1 square micron each one

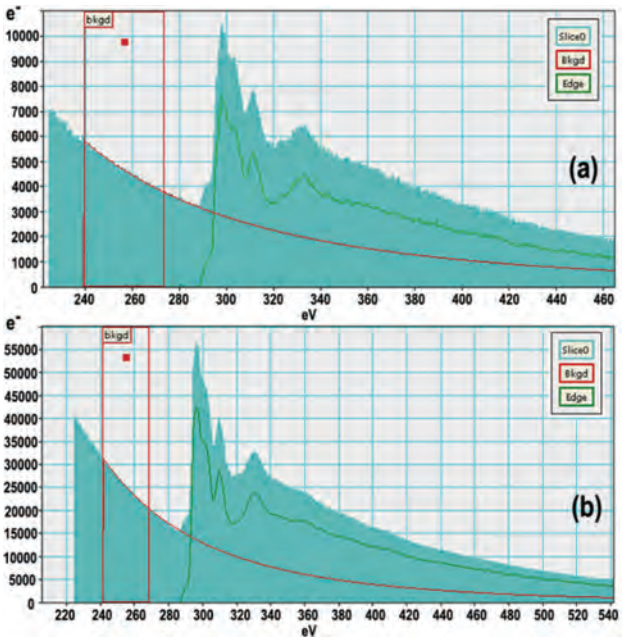

Figure 4. Electron Energy Loss Spectroscopy (EELS) (a) DND, (b) LND.

were analyzed. All results indicated much higher purity of LND sample.

4.4. Raman and Photo-Luminescence Spectroscopy

Spectroscopic properties of nanodiamonds are determined by their structure. So, Raman and luminescence can be used for the detecting interaction of nanodiamonds with bio-objects,[34, 35] as well as for the estimation of their performance. The origin of HTHP ND luminescence

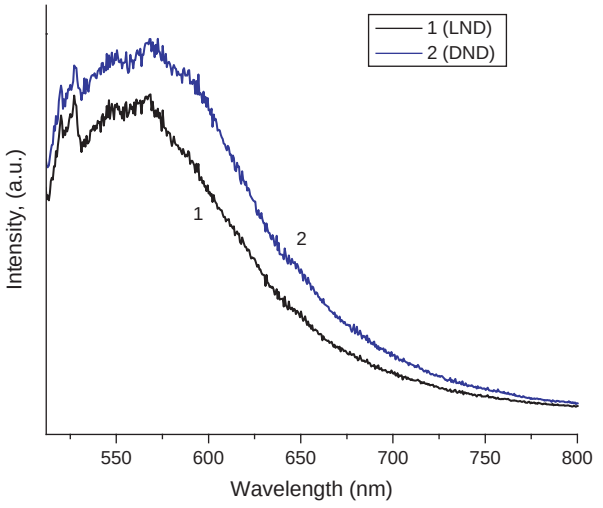

Figure 6. Luminescence spectra of LND (1) and DND (2).

important for bio-imaging is mostly nitrogen vacancy centers and the methods to increase their number have been developed,[36] while the nature of DND luminescence, apparently caused by defects and admixtures in diamond structure,[15] is still discussed.[36, 37]

Raman spectra were measured for the samples on Si substrate, using confocal micro-spectrometersα-SNOM (Witec, Germany) withexcitations 488 nm and T64000 (Horiba JobinYvon, France) with excitations 325 nm, laser power in the focal spot was 1 mW. The luminescence spectra were obtained with excitation 488 nm (α-SNOM, Witec).

The luminescence of studied samples at the excitation of 488 nm reveals wide peak centered about 565 nm (Fig. 6).

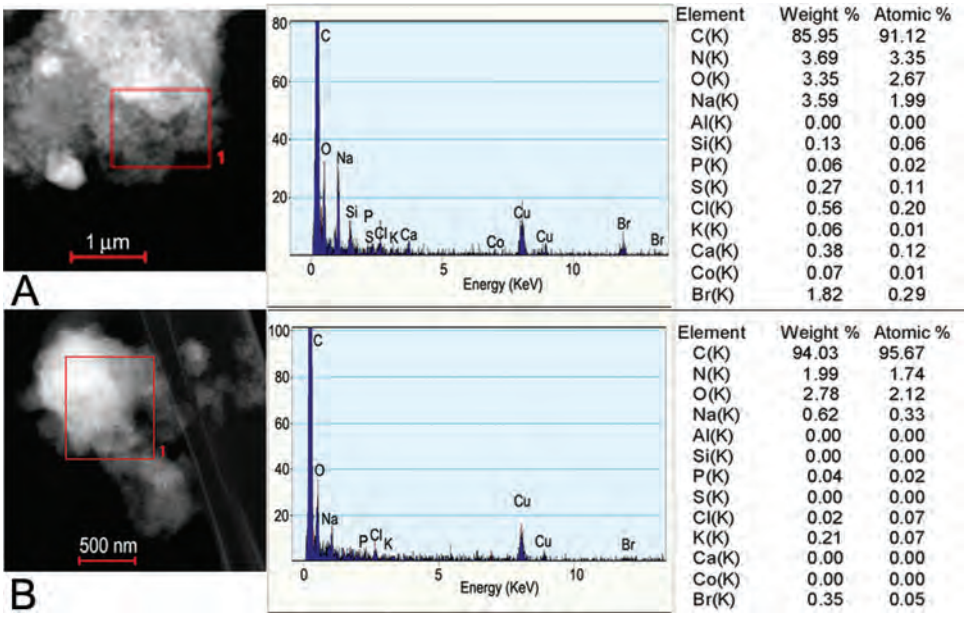

Figure 5. Energy Dispersive X-Ray Spectroscopy (EDS) (a) DND, (b) LND, the analyzed area (left), energy Dispersive X-Ray Spectra (middle) and elements quantity (right).

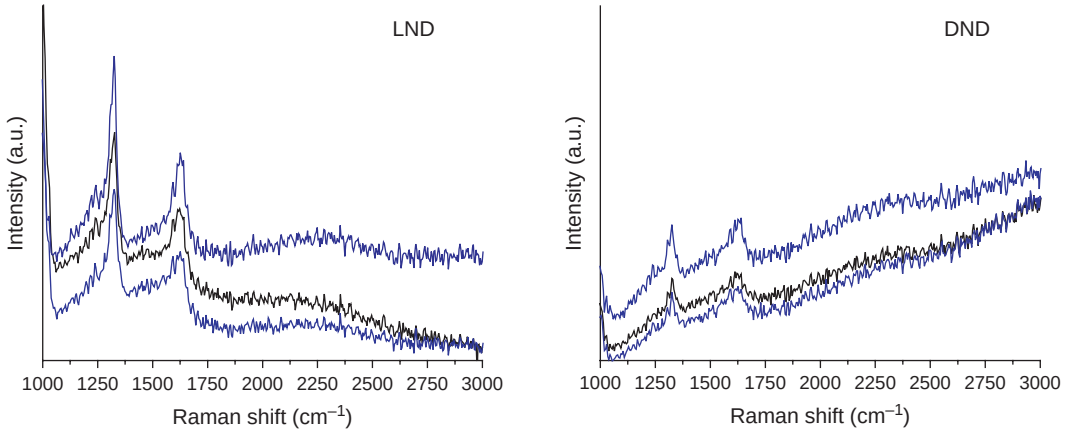

Figure 7. Raman shift of LND (left) and DND (right) at excitation 488 nm.

The observed weak luminescence is quite characteristic for the luminescence of nanodiamonds with crystallite size 3–10 nm.[14] Luminescence of LND and DND samples is similar in intensity and peak shape. This kind of ND luminescence can be related to emission from electron levels created in the diamond band gap by surface defects.[37] Note that luminescence is low but detectable. Also, good diamond structure of crystallites (discussed above in accordance with results of Raman spectroscopic analysis) presumably allows discussion of further increasing of the fluorescence intensity. The same spectra also reveal the peaks which are originated from nanodiamond Raman scattering.

Raman spectra (Fig. 7) were measured at excitations 488. The spectra of both samples contain two main lines at 1325 and 1630 cm^{-1} usually related to the phonon modes of sp^3 (diamond) and sp^2-bonded (graphite G-peak) carbon. The diamond Raman peak is normally positioned at 1332 cm^{-1}, but with the crystallites size decreasing to a few nm the diamond peak is shifted to lower wavenumbers and broadens due to the phonon confinement effect.[38] As for strong shift of G-peak from 1590 cm^{-1} to 1630 cm^{-1} and above, it can be assigned to a superposition of sp^2 carbon band at 1590 cm^{-1} with a peak of O—H bending vibrations at 1640 cm^{-1}. C=O stretching vibrations, which are shown to be positioned at 1740 cm^{-1} in the Raman spectrum of oxidized ND, produce a shoulder on the 1640 cm^{-1} peak.[39] Thus, obtained Raman spectra are in correspondence with results of Fourier Transform Infrared Spectroscopy investigation of LND, presented in Ref. [40]. Together with size, the Raman spectra give also information about surface groups.

In the Raman spectrum of LND the relative intensity of diamond is higher than one for DND. As the cross-section of Raman scattering of graphite is much higher than diamond,[41] the predominance of diamond peak confirms high content of diamond phase.[6] It can give some advantages for LDN nanoparticles bio-applications, due to more convenient properties of diamond in comparison with graphite (better structural and spectroscopic properties and better controllable surface properties),[42] while the properties of DND and graphite nanoparticles of comparable size are also comparable.[43, 44]

In Raman spectra of LND together with lines near 1325 and 1630 cm^{-1}, the line at 1445 cm^{-1} of low intensity can be observed. This line in carbon nanostructured materials can be observed and its origin is discussed: the peak 1450 cm^{-1} as well as peak at 1120–1150 cm^{-1} are speculatively due to carbon–hydrogen bonds in the grain boundaries[45] or transpolyacetelens, also on nanodiamond surface.[46] Other explanation is connected with size effect originated from the presence of confined phonon modes in diamond.[47] Also, additionally to down-shift of Raman diamond peak for nanodiamonds of size about a few nm, the peak is broadened, with a shoulder at 1250 cm^{-1} that originates from smaller nanodiamond particles or smaller coherent scattering domains separated by defects in larger nanodiamond particles.[48]

4.5. Purity Determination

EDS analysis described earlier and arithmetic average calculation allow to conclude, that the DND sample without any pretreatment contains 85.95 wt. % carbon, while LND one contains 94.03 wt. %.

Since EDS analysis can give just some indication on the purity of the analyzed samples, the additional testing was conducted to determine the incombustible residue of nanodiamond powders. The incombustible residue of 0.5 wt. % found in DND sample indicates high purity of the analyzed DND powder comparing with the existing on the market products, which usually have incombustible residue more than 1 wt. %.[49] In the case of LND sample incombustible residue has not been detected at all, which confirms the highest purity of LND powder (the sensitivity of the measuring was 0.02 wt. %). This is caused by the method of synthesis, in which the raw material is a compound containing the carbon black and hydrocarbons free of metallic impurities.

5. ANALYSIS OF NANODIAMONDS INFLUENCE ON THE IMMUNE SYSTEM

Nanodiamonds offer a unique combination of biologically relevant properties providing possible advantages over other nanoparticles. In recent years nanodiamonds have been explored for use in wide range of bio-medical applications particularly in cancer therapy and gene delivery.[6–8] A primary requirement for biomedical carriers is their compatibility to the biological environment. Previous *in-vitro* studies have demonstrated that nanodiamonds are not cytotoxic in neuroblastoma and macrophage cell lines.[50] Subsequently the cytotoxicity of nanodiamonds with different sizes and surface properties was studied by several research groups. It was found that nanodiamonds in complete cell culture media are mostly non-cytotoxic for HeLa cells and cytotoxicity of nanodiamonds depends on serum proteins present in the cell culture medium.[51] *In-Vivo* Toxicity study has been found that nanodiamonds have no or a small toxic side effect on biological systems, however metabolism of nanodiamonds may be different under various conditions.[52]

In this study a possible influence of DND and LND on the immune system has been investigated *in vitro* in a culture system containing two cell lines: RAW 264 (mouse Macrophage cell line) and TK-1 (T-cell leukemia). TK-1 mouse cells were incubated for 2 hours with the same concentrations of DND at the first and LND in the second group, whereupon the immune response of lymphocytes CD69 and CD25 has been analyzed in accordance to previously reported method.[53] The representative flow cytometry histograms are presented (Fig. 8). DND histograms show the log shift, which means that DND particles induce lymphocyte activation, while, in contrast, at application of LND shift is the same like control CD69 and CD25 lymphocytes.

Isotope control (antibodies that did not recognize the CD25 or CD69) gave similar result indicating that LND did not activate lymphocytes. In addition, it was found that DND induce much more proinflammatory cytokines (IL-2, IL-12p40, TNF, and IFN gamma) compared to LND (data not shown) in macrophage cell line (Raw 264.7) which indicates a potential toxicity of DND.

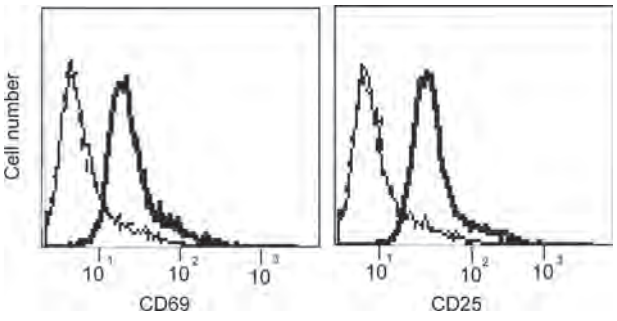

Figure 8. Representative flow cytometry histograms. LND: regular line, DND: bold line.

To be sure that LND do not initiate an immune response (mainly not a pro-inflammatory response) and can be defined as the safe material for biomedical applications, additional *in vitro* assays should be performed, particularly a complement activation in human serum, interferon response assays and coagulation cascade assays. In addition, a panel of *in vivo* assays should be performed in order to determine no immune toxicity of LND.

In addition to the immune system, liver enzyme release and global changes in body weight should be measured. These simple assays will provide insightful information about the biocompatibility of LNDs in biomedical applications.

6. CONCLUSIONS AND PROSPECTS

New technology for producing nanodiamonds by laser treatment of specially prepared target containing carbon source has been developed. In general LHDP technology enables to vary the size of synthesized nanodiamonds[41,54] and to obtain LND of high purity practically free of metals. In contrast to the existing non-controllable technologies for nanodiamonds manufacturing, LHDP enables to provide the diamond nanopowder with constant properties especially important for producing nanodiamond dispersions in physiological solvents with high sedimentation stability in wide range of temperatures and acidity levels. The possibility to control the levels of photoluminescence and paramagnetism during the synthesis should be tested in further investigation.

The comparative analysis of LND and DND samples shows that LND and DND have similar structure and particle size (about 4–5 nm) and indicate some advantages of LND highly important for bio-applications: higher purity, better structural and spectroscopic properties, higher paramagnetism,[53] easier control of surface chemistry (due to the absence of metal and graphite impurities) and lower cytotoxicity. In contrast to the investigated DND sample, LND one has not induced lymphocytes activation *in vitro* in a culture system. Further research should aim at LND surface modification with antibodies and their examination *in vitro* and *vivo* activity.

References and Notes

1. V. V. Danilenko, *Phys. Solid State* 46, 595 **(2004)**.
2. W. Gu, N. Peters, and G. Yushin, *Carbon* 53, 292 **(2013)**.
3. M. Y. Shalaginov, S. Ishii, J. Liu, J. Liu, J. Irudayaraj, A. Lagutchev, A. V. Kildishev, and V. M. Shalaev, *Appl. Phys. Lett.* 102, 173114 **(2013)**.
4. N. N. Vershinin, O. N. Efimov, V. A. Bakaev, A. E. Aleksenskii, M. V. Baidakova, A. A. Sitnikova, and Vul' A. Ya, *Nanotubes and Carbon Nanostructures* 19, 63 **(2010)**.
5. V. A. Gerasin, E. M. Antipov, V. V. Karbushev, V. G. Kulichikhin, G. P. Karpacheva, R. V. Talroze, and Y. V. Kudryavtsev, *Russ. Chem. Rev.* 82, 303 **(2013)**.
6. V. N. Mochalin, O. Shenderova, D. Ho, and Y. Gogotsi, *Nature Nanotech.* 7, 711 **(2012)**.

7. E. Osava and D. Ho, *J. Med. Allied Sci.* 2, 31 **(2012)**.
8. A. Krueger, *J. Mater. Chem.* 21, 12571 **(2011)**.
9. E. Perevedentseva, Y.-C. Lin, Mona Jani, and C.-L. Cheng, *Future Medicine Nanomedicine* 8, 2041 **(2013)**.
10. Y. Y. Hui, B. Zhang, Y. C. Chang, C. C. Chang, H. C. Chang, J. H. Hsu, K. Chang, and F. H. Chang, *Optics Express* 18, 5896 **(2010)**.
11. R. Igarashi, Y. Yoshinari, H. Yokota, T. Sugi, F. Sugihara, K. Ikeda, H. Sumiya, S. Tsuji, I. Mori, H. Tochio, Y. Harada, and M. Shirakawa, *Nanolett.* 12, 5726 **(2012)**.
12. Q. Zhang, V. N. Mochalin, I. Neitzel, I. Y. Knoke, J. Han, C. A. Klug, J. G. Zhou, P. I. Lelkes, and Y. Gogotsi, *Biomaterials* 32, 87 **(2011)**.
13. "HPHT synthesis." International Diamond Laboratories. Retrieved 2009–05–05.
14. P. H. Chung, E. Perevedentseva, and C. L. Cheng, *Surf. Sci.* 601, 3866 **(2007)**.
15. A. Shiryaev, K. Iakoubovskii, D. Grambole, N. Dubrovinskaia, and J. Phys, *Condens. Matter.* 18, L493 **(2006)**.
16. A. Krueger and D. Lang, *Adv. Funct. Mater.* 22, 890 **(2012)**.
17. Y. C. Lin, E. Perevedentseva, L. W. Tsai, K. T. Wu, and C. L. Cheng, *J. Biophotonics* 5, 838 **(2012)**.
18. X. Xu, Y. Zhu, B. Wang, Z. Yu, and S. Xie, *J. Mater. Sci. Technol.* 21, 496 **(2005)**.
19. A. Kruger, F. Kataoka, M. Ozava, T. Fujino, Y. Suzuki, A. Aleksenskii, A. Vul, and E. Osawa, *Carbon* 43, 1722 **(2005)**.
20. E. Osawa, Synthesis and Applications of Ultrananocrystalline Diamond, edited by D. M. Gruen, O. Shenderova, and A. Vul, Springer, Netherlands **(2005)**, p. 231.
21. A. Ya. Vul, A. T. Dideikin, Z. G. Tsareva, M. N. Korytov, P. N. Brunkov, B. G. Zhukov, and S. I. Rozov, *Tech. Phys. Lett.* 32, 561 **(2006)**.
22. K. Xu and Q. Xue, *Phys. Solid State* 46, 633 **(2004)**.
23. E. Osawa, *Pure Appl. Chem.* 80, 1365 **(2008)**.
24. Y. Liang, M. Ozawa, and A. Krueger, *ACS Nano* 3, 2288 **(2009)**.
25. H. Zeng, X. W. Du, S. C. Singh, S. A. Kulinich, S. Yang, J. He, and W. Cai, *Adv. Funct. Mater.* 22, 1333 **(2012)**.
26. P. P. Patil, D. M. Phase, S. A. Kulkarni, S. V. Ghaisas, S. K. Kulkarni, S. M. Kanetkar, S. B. Ogale, and V. G. Bhide, *Phys. Rev. Lett.* 58, 238 **(1987)**.
27. G. W. Yang, J. B. Wangand, and Q. X. Liu, *Phys.: Condens. Matter* 10, 7923 **(1998)**.
28. G. A. Askar'yan, A. M. Prokhorov, G. Chanturiya, and G. P. Shipulo, *Soviet Physics JEPTr* 17, 1463 **(1963)**.
29. G. A. Askar'yan, *JETP Lett.* 4, 99 **(1966)**.
30. R. Y. Chiao, E. Garmire, and C. H. Townes, *Phys. Rev. Lett.* 13, 479 **(1964)**.
31. V. Uvarov and I. Popov, *Mater. Charact.* 85, 111 **(2013)**.
32. I. I. Vlasov, O. Shenderova, S. Turner, O. I. Lebedev, A. A. Basov, I. Sildos, M. Rahn, A. A. Shiryaev, and G. Van Tendeloo, *Small* 6, 687 **(2010)**.
33. L. W. Finger, D. E. Cox, and A. P. Jephcoat, *J. Appl. Cryst.* 27, 892 **(1994)**.
34. R. Kaur and I. Badea, *Int. J. Nanomed.* 8, 203 **(2013)**.
35. J. M. Say, C. van Vreden, D. J. Reilly, L. J. Brown, J. R. Rabeau, and N. J. C. King, *Biophys. Rev.* 3, 171 **(2011)**.
36. S. J. Yu, M. W. Kang, H. C. Chang, K. M. Chen, and Y. C. Yu, *J. Am. Chem. Soc.* 127, 17604 **(2005)**.
37. J. P. Boudou, P. A. Curmi, F. Jelezko, J. Wrachtrup, P. Aubert, M. Sennour, G. Balasubramanian, R. Reuter, A. Thorel, and E. Gaffet, *Nanotechnology* 20, 235602 **(2009)**.
38. S. Osswald, V. N. Mochalin, M. Havel, G. Yushin, and Y. Gogotsi, *Phys. Rev. B* 80, 075419 **(2009)**.
39. V. Mochalin, S. Osswald, and Y. Gogotsi, *Chem. Mater.* 21, 273 **(2009)**.
40. M. V. Baidakova, Yu. A. Kukushkina, A. A. Sitnikova, M. A. Yagovkina, D. A. Kirilenko, V. V. Sokolov, M. S. Shestakov, A. Ya. Vul', B. Zousman, and O. Levinson, *Phys. Solid State* 55, 1747 **(2013)**.
41. R. J. Nemanich, J. T. Glass, G. Lucovsky, and R. E. Sroder, *J. Vac. Sci. Technol. A,* 6, 1783 **(1988)**.
42. A. S. Barnard, *Analyst.* 134, 1751 **(2009)**.
43. M. Wierzbicki, E. Sawosz, M. Grodzik, M. Prasek, S. Jaworski, and A. Chwalibog, *Nanoscale Res. Let.* 8, 195 **(2013)**.
44. M. Wierzbicki, E. Sawosz, M. Grodzik, A. Hotowy, M. Prasek, S. Jaworski, F. Sawosz, and A. Chwalibog, *Int. J. Nanomed.* 8, 327 **(2013)**.
45. J. Birrell, J. E. Gerbi, O. Auciello, J. M. Gibson, J. Johnson, and J. A. Carlisle, *Diamond Relat. Mater.* 14, 86 **(2005)**.
46. A. C. Ferrari and J. Robertson, *Phil. Trans. R. Soc. Lond. A* 362, 2477 **(2004)**.
47. A. T. Sowers, B. L. Ward, S. L. English, and R. J. Nemanich, *J. Appl. Phys.* 86, 3973 **(1999)**.
48. S. Osswald, G. Yushin, V. Mochalin, S. O. Kucheyev, and Yu. Gogotsi, *J. Am. Chem. Soc.* 128, 11635 **(2006)**.
49. N. V. Novikov and G. P. Bogatyreva, *Journal of Superhard Materials* 30, 73 **(2008)**.
50. A. M. Schrand, H. Huang, C. Carlson, J. J. Schlager, E. O. Sawa, S. M. Hussain, and L. J. Dai, *Phys. Chem. B* 111, 2 **(2007)**.
51. Y. Zhu, J. Li, W. Li, Y. Zhang, X. Yang, N. Chen, Y. Sun, Y. Zhao, C. Fan, and Q. Huang, *Theranostics* 2, 302 **(2012)**.
52. Y. Xing, W. Xiong, L. Zhu, E. Osawa, S. Hussin, and L. Dai, *ACS Nano* 5, 2376 **(2011)**
53. D. Peer, P. Zhu, C. V. Carman, J. Lieberman, and M. Shimaoka, *Proc. Natl. Acad. Sci. USA* 104, 4095 **(2007)**.
54. A. M. Panich, A. I. Shames, B. Zousman, and O. Levinson, *Diamond Relat. Mater.* 23, 150 **(2012)**.

Received: 11 November 2013. Accepted: 3 January 2014